Quantum Simulation of $\mathbb{Z}_2$ Lattice Gauge theory with minimal resources

Reinis Irmejs, Mari-Carmen Banuls, and J. Ignacio Cirac
Max-Planck-Institut für Quantenoptik, Hans-Kopfermann-Str. 1, D-85748 Garching, Germany and
Munich Center for Quantum Science and Technology (MCQST), Schellingstr. 4, D-80799 Munich, Germany
(Dated: June 17, 2022)

The quantum simulation of fermionic gauge field theories is one of the anticipated uses of quantum computers in the NISQ era. Recently work has been done to simulate properties of the fermionic $\mathbb{Z}_2$ gauge field theory in (1+1)D and the pure gauge theory in (2+1) D. In this work, we investigate various options for simulating the fermionic $\mathbb{Z}_2$ gauge field theory in (2+1) D. To simulate the theory on a NISQ device it is vital to minimize both the number of qubits used and the circuit depth. In this work we propose ways to optimize both criteria for simulating time dynamics. In particular, we develop a new way to simulate this theory on a quantum computer, with minimal qubit requirements. We provide a quantum circuit, simulating a single first order Trotter step, that minimizes the number of 2-qubit gates needed and gives comparable results to methods requiring more qubits. Furthermore, variational Trotterization approaches are investigated that allow to further decrease the circuit depth.

I. INTRODUCTION

Simulating the dynamics of physical quantum systems is one of the most anticipated applications of quantum computing and a good candidate to show useful quantum advantage for a NISQ device [1]. Physical systems of interest include quantum chemistry models, material simulations, and high energy physics problems via lattice gauge theories, as the one considered here [2–4]. To simulate the quantum dynamics on a near-term quantum device, the resources used need to be optimized. NISQ devices offer only a limited number of qubits, and have limited coherence times, as well as considerable 2-qubit gate errors [5]. Thus, to simulate a given problem it is necessary to optimize the number of qubits used and their architecture, as well as the depth (and the number of 2-qubit gates) of the quantum circuit.

In this work, we focus on the simulation of the fermionic $\mathbb{Z}_2$ lattice gauge theory in 2+1D with minimal resources. In particular, we use as benchmarks the number of qubits and of 2-qubit quantum gates needed to implement a single first-order Trotter step. The latter can be used to probe the dynamics of the system either directly, via a Trotterised time evolution, or by using it as a single step for an ansatz to perform variational quantum algorithms for time evolution, like parametrised variational quantum dynamics (pVQD) [6–8]. The same ansatz can also be applied for other algorithms like QAOA or variational quantum eigensolver (VQE) to probe the ground state properties. In minimizing the resources needed, we exploit the fermion mapping introduced in [9, 10], which allows the fermionic $\mathbb{Z}_2$ theory to be encoded with the same number of qubits as the pure gauge theory without the fermions. This is the first practical proposal that evaluates the resources needed for simulating such fermionic (2+1) D physical system on a quantum computer [1]. We compare the circuit depth obtained via fermion elimination method with that if a standard approach like Verstraete-Cirac (VC) [12] transformation was used to encode the fermionic degrees of freedom. The new method offers similar circuit depth requirements (18 to 14 CX gates per link), while only using half of the qubits compared to the VC encoding. Furthermore, the use of variational pVQD algorithm is explored to further reduce the requirements for the circuit depth to perform time evolution of the system.

High energy physics models have been simulated with great success by discretizing the theory on a lattice [13, 14]. In this work, the $\mathbb{Z}_2$ lattice gauge theory with fermions was picked due to its simplicity and for the ease of encoding the gauge field in qubits, nevertheless the theory is also of practical interest. In high energy physics, SU(N) theories are of particular importance, since the strong force, responsible for quark binding and their interactions is mediated via SU(3) gauge field. The exact mechanism of the quark confinement is poorly understood and many insights have been obtained from numerical simulations. In particular, it is believed that the centre of the SU(N) theory - Z(N) is responsible for the confinement [15]. However, classical simulations using Monte-Carlo methods suffer from a sign problem and scale exponentially in the resources with the system size. By using quantum computers it could be possible to avoid this problem by working in the Hamiltonian formalism. We show that the circuit depth needed to simulate a single Trotter step is independent of the system size, allowing the simulation to be scaled. As the quantum technologies continue to advance, it is important to explore the optimal ways to simulate this theory in a sign problem free way to better understand its properties, and eventually the process of quark confinement. This work only considers the $\mathbb{Z}_2$ theory, but the methods used here

[1] While completing this manuscript, an independent proposal has appeared that explored the use of the same fermion elimination method and also considered the fermionic $\mathbb{Z}_2$ theory in (2+1) D in their work [11]

can be altered to probe other $\mathbb{Z}_N$ theories, which are left for future work.

Previous work in [16–18] covered the simulation of a pure $\mathbb{Z}_2$ theory in (2+1) D. Very recently, [19] simulated the fermionic $\mathbb{Z}_2$ theory in 1+1D, with an implementation on the Google Sycamore quantum device, and particular emphasis on probing the confinement. The authors were able to perform the simulation of time dynamics via Trotterization, with a much greater accuracy than one naively would expect from the 2-qubit gate error rate of the device. These works point out the current interest of simulating the full fermionic $\mathbb{Z}_2$ theory in (2+1) D, which we tackle in this paper.

In the first part of this article we consider the pure gauge and fermionic $\mathbb{Z}_2$ theory in (2+1)D along with the work that has been done so far. Next we introduce the mechanism to encode the fermions in the gauge-field, as proposed in [9, 10], and how it can be applied to the $\mathbb{Z}_2$ theory. In section III, we show how this model can be mapped to a quantum circuit and evaluate the necessary number of 2-qubit gates needed for a single step of a first order Trotter circuit, which is compared with the VC method. Section IV explores the use of the variational methods, including numerical results. Finally, section V summarizes our conclusions.

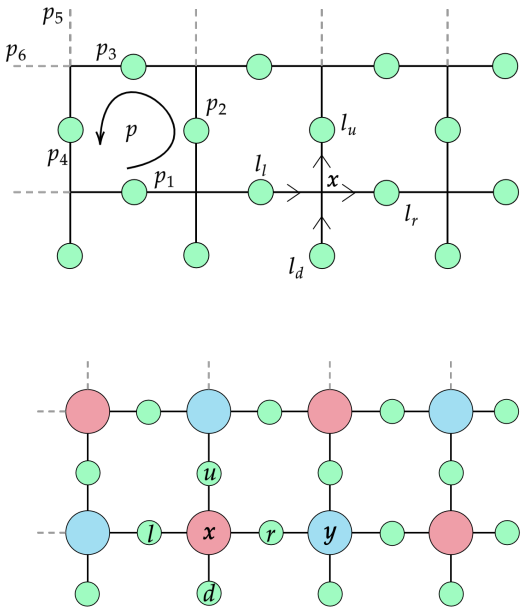

FIG. 1: The top figure shows the labelling for the pure gauge theory on a lattice. The bottom figure shows the labelling for the full fermionic theory with staggered fermionic matter. Matter sites are located on vertices while gauge fields are on the links.

II. $\mathbb{Z}_2$ LATTICE GAUGE THEORY

In the lattice gauge theory Hamiltonian formalism, the space is discretized, but the time is left continuous. On the lattice, matter fields are located on the vertices (labelled by vectors $\boldsymbol{x}$) and the gauge fields on the links (labelled l) connecting them. When considering the fermionic $\mathbb{Z}_2$ lattice gauge theory in two spatial dimensions, the fermions can be staggered as shown in figure 1—on even sites (red) we have particles and on the odd sites (blue)—antiparticles with charges +1 and -1. The parity of the site is given by $(-1)^{s(\boldsymbol{x})} = (-1)^{x+y}$ with 1 (-1) indicating an even (odd) site [20]. The green sites on the links denote the gauge fields. We will consider two-dimensional rectangular lattices with periodic boundary conditions and dimension $M \times N$, where M, N are even, to accommodate fermion staggering. Note that on a lattice of size $M \times N$, there are $L = 2 \times M \times N$ gauge field links and $M \times N$ fermion vertices (Fig 1). The gauge field in $\mathbb{Z}_N$ theories has a finite-sized Hilbert space of dim = N, thus allowing it to be encoded on each link.

A. Pure $\mathbb{Z}_2$ lattice gauge theory

The Kogut-Susskind Hamiltonian of the pure gauge $\mathbb{Z}_2$ theory is given by H_{KS} [21]

$$H_{KS} = H_E + H_B \tag{1}$$
$$= \lambda_E \sum_l [2 - (P_l + P_l^\dagger)] \tag{2}$$
$$+ \lambda_B \sum_p [2 - (U_{p_1} U_{p_2} U_{p_3}^\dagger U_{p_4}^\dagger + H.c.)]. \tag{3}$$

For the electric field term H_E the sum is over all links and for the magnetic field term H_B over all plaquettes p, as indicated in the Fig 1. The coupling constants are connected through the relations $\lambda_E = g^2/2$, $\lambda_B = 2/g^2$ [21]. An additional constraint that the theory obeys is the Gauss law:

$$\begin{aligned} G(x) &= P_u P_r P_d^\dagger P_l^\dagger \\ &= \exp(i\pi[E_u + E_r - E_d - E_l]) \\ &= \exp(i\pi Q(\boldsymbol{x})) = 1 \end{aligned} \tag{4}$$

where $Q(\boldsymbol{x})$ is the charge on vertex $\boldsymbol{x}$. or the pure gauge theory with no static charges $Q(\boldsymbol{x}) = 0$ on all sites. The sign convention for the electric fields is given in Fig. 1.

In the pure $\mathbb{Z}_2$ lattice gauge theory the electric field can take two values: 0 and 1. The theory can be defined using

two generators U_l, P_l per link l, satisfying the relations

$$P_l^2 = U_l^2 = 1 \tag{5}$$

$$P_l^\dagger P_l = U_l^\dagger U_l = 1 \tag{6}$$

$$P_l^\dagger U_l P_l = \exp(i\pi U_l) \tag{7}$$

The gauge field on a given link can be encoded into qubit states $|0\rangle, |1\rangle$ corresponding to the electric field values such that $U_l |E\rangle = |(E+1) \mod 2\rangle$ and $P_l |E\rangle = \exp(i\pi E) |E\rangle$. Thus, U_l is the raising operator for the gauge field and P_l is a diagonal operator in this basis, describing the electric field strength.

This Hamiltonian can be implemented on a quantum computer by mapping:

$$U_l \to X_l \tag{8}$$

$$P_l \to Z_l, \tag{9}$$

where (X_l, Y_l, Z_l) are Pauli matrices acting on link l. The Kogut-Susskind Hamiltonian is expressed as:

$$H_{KS} = H_E + H_B \tag{10}$$

$$= -2\lambda_E \sum_l Z_l - 2\lambda_B \sum_p X_{p_1} X_{p_2} X_{p_3} X_{p_4}, \tag{11}$$

and the Gauss law (in the absence of external charges) is given by

$$Z_u Z_r Z_d Z_l = 1 \tag{12}$$

for every vertex. The quantum circuit to simulate this model will be explicitly shown in the next section.

B. Fermionic $\mathbb{Z}_2$ lattice gauge theory

In the full theory, when the gauge field interacts with matter, the Hamiltonian acquires two extra terms, the mass term of the dynamical fermions and the interaction term between the fermions and the gauge field. The matter field part of the Hamiltonian is given by:

$$H_f = H_M + H_{int} \tag{13}$$

$$= \sum_x (-1)^{s(\boldsymbol{x})} M a_{\boldsymbol{x}}^\dagger a_{\boldsymbol{x}} \tag{14}$$

$$+ \epsilon \sum_{\boldsymbol{x}} a_{(x,y)}^\dagger U_r(\boldsymbol{x}) a_{(x+1,y)} + H.c. \tag{15}$$

$$+ \epsilon \sum_{\boldsymbol{x}} a_{(x,y)}^\dagger U_u(\boldsymbol{x}) a_{(x,y+1)} + H.c. \tag{16}$$

with $a_i, a_j^\dagger$ satisfying the canonical anticommutation relations (CAR). Note that the interaction term has been split into horizontal and vertical parts for future convenience. To accommodate both particles and antiparticles on the lattice, the staggered fermion approach is used. Here on even (odd) sites we have particles (antiparticles) with charge +1 (-1). The parity of the site $\boldsymbol{x} = (x, y)$ is given by $(-1)^{s(\boldsymbol{x})} = (-1)^{x+y}$ with 1 (-1) indicating an even (odd) site. In this approach, in the computational basis,

$$\text{on even site} \begin{cases} |0\rangle \to \text{ vacuum (no charge)} \\ |1\rangle \to \text{ particle (charge +1)} \end{cases} \tag{17}$$

$$\text{on odd site} \begin{cases} |0\rangle \to \text{ anti-particle (charge -1)} \\ |1\rangle \to \text{ vacuum (no charge)} \end{cases}$$

The number operator on the vertex is given by:

$$n(\boldsymbol{x}) = \frac{1 - (-1)^{s(\boldsymbol{x})} Z_x}{2}. \tag{18}$$

While the number operator can be easily expressed, getting the fermionic creation/annihilation operators is non-trivial, as they obey the non-local CARs. In the method from [9, 10], introduced in the next section, the fermionic statistics is absorbed into the gauge field, at the expense of increasing the Pauli weight of the Hamiltonian terms (i.e. the number of qubits on which the term acts non-trivially). The transformed Hamiltonian consists of hard-core bosonic matter for which creation/annihilation operators can be implemented with simple spin raising/lowering ones. Furthermore, these hard-core bosonic degrees of freedom can be eliminated by the use of Gauss law, which uniquely determines the charge distribution on the vertices. This allows the full fermionic $\mathbb{Z}_2$ theory to be simulated with the same number of qubits as needed for the pure gauge one, minimizing the spatial resources of the quantum computation.

C. Fermion encoding via elimination

In [9] a method is introduced that allows one to perform a unitary transformation that converts the fermionic degrees of freedom to hard core bosonic degrees of freedom, if the gauge group has $\mathbb{Z}_2$ as a normal subgroup. As a result, the theory acquires phase factors ξ of the gauge field to keep track of the fermionic exchange antisymmetry. The transformed Hamiltonian is

$$H_M = \sum_x (-1)^{s(\boldsymbol{x})} M \eta_{\boldsymbol{x}}^\dagger \eta_{\boldsymbol{x}} \tag{19}$$

$$H_{KS} = -\lambda_E \sum_l (P_l + P_l^\dagger) - \lambda_B \sum_p (\xi_p U_{p_1} U_{p_2} U_{p_3}^\dagger U_{p_4}^\dagger + H.c.) \tag{20}$$

$$H_I = -i\epsilon \sum_{\boldsymbol{x}} \xi_h(\boldsymbol{x}) \eta_{(x,y)}^\dagger U_r(\boldsymbol{x}) \eta_{(x+1,y)} + H.c. \tag{21}$$

$$- i\epsilon \sum_{\boldsymbol{x}} \xi_v(\boldsymbol{x}) \eta_{(x,y)}^\dagger U_u(\boldsymbol{x}) \eta_{(x,y+1)} + H.c. \tag{22}$$

where $\eta(\boldsymbol{x})$ is a staggered hard-core boson annihilation operator and the ξ phase factors are given by:

$$\xi_h(x,y) = (-1)^{E_u(x,y)+E_l(x,y)+E_d(x,y)+E_d(x+1,y)} \quad (23)$$

$$\xi_v(x,y) = (-1)^{E_l(x,y)+E_d(x,y)} \quad (24)$$

$$\xi_p = (-1)^{E_{p_1}+E_{p_2}+E_{p_5}+E_{p_6}} \quad (25)$$

and the ordering is shown in the Fig 1. Under this transformation, the Gauss' law remains unchanged. This is important, as the Gauss' law fully defines the charge configuration on the vertex and thus can be used to eliminate the matter fields [10].

For an occupied (unoccupied) site ($n(x) = 1(0)$) $Q(x) = \pm 1(0)$ and the Gauss' law gives $P_u P_r P_d^\dagger P_l^\dagger = -1$ (1). This allows us to define projection operators $\Pi_\rho(x,y)$ that project the Hilbert space to the subspace with $G(x) = \rho$, with $\rho = 1$ indicating that the site is empty and $\rho = -1$ that the site is full.

Elimination of the matter fields via Gauss law leads to the H_f terms to acquire projection operators as follows:

$$H_f = H_M + H_{int} \quad (26)$$

$$= \sum_{\boldsymbol{x}} M\Pi_{-1}(\boldsymbol{x}) \quad (27)$$

$$- i\epsilon \sum_{\boldsymbol{x}} (-1)^{s(\boldsymbol{x})} \xi_h(\boldsymbol{x}) \Pi_{-1}(x,y) U_r(x,y) \Pi_1(x+1,y) + H.c. \quad (28)$$

$$- i\epsilon \sum_{\boldsymbol{x}} (-1)^{s(\boldsymbol{x})} \xi_v(\boldsymbol{x}) \Pi_{-1}(x,y) U_u(x,y) \Pi_1(x,y+1) + H.c. \quad (29)$$

where the factors of $(-1)^{s(\boldsymbol{x})}$ arise from fermion staggering. Thus, the full fermionic $\mathbb{Z}_2$ theory can be simulated only by encoding the gauge field values. Once again, it is worth re-emphasizing that the matter fields have been eliminated at the expense of the Gauss' law, thus leaving the new theory without this constraint.

To perform such a simulation on a quantum computer, one has to implement the non-trivial projection operators. In further sections it will be shown how each of these terms can be encoded on a digital quantum computer.

D. Full $\mathbb{Z}_2$ theory as a spin system

The Hamiltonian without the matter sites can be mapped to operators on a quantum computer. We will assume access to Pauli gates (X, Y, Z) and their rotations $R_x(\theta), R_y(\theta), R_z(\theta)$ as well as controlled Pauli gates and their rotations as the 2 qubit gates. To implement this model, it is necessary to have an architecture of qubits with a possibility to perform a 2 qubit gate with next-to-nearest neighbours.

In order to perform the simulation, in addition to the mapping of $U_l \to X_l$ and $P_l \to Z_l$ introduced previously, we need to map the projection operators Π_g and the phase factors ξ. The mapping of the phase factors is straight forward since $(-1)^{E_l} = P_l$. The projection operator Π_ρ can be implemented as follows:

$$\Pi_{\pm 1}(x,y) = \frac{1}{2}(1 \pm Z_u Z_l Z_d Z_r(x,y)) = \frac{1}{2}(1 \pm G(x,y)) \quad (30)$$

The Hamiltonian mass term H_M is thus given by:

$$H_M = \sum_x \frac{M}{2}(1 - Z_u Z_r Z_d Z_l) \quad (31)$$

Since we know how to implement each operator in the interaction Hamiltonian H_{int}, it can be mapped to a quantum device. While the structure of it looks complicated, it is possible to simplify it quite a lot. Consider the horizontal part of the interaction Hamiltonian and note that $U = U^\dagger = X$

$$\begin{aligned}
H_H &= -i\epsilon \sum_{\boldsymbol{x}} (-1)^{s(\boldsymbol{x})} \xi_h(\boldsymbol{x}) \Pi_{-1}(x,y) U_r(x,y) \Pi_1(x+1,y) + H.c. \\
&= -i\epsilon \sum_{\boldsymbol{x}} (-1)^{s(\boldsymbol{x})} U_r(x,y) \xi_h(\boldsymbol{x}) \Pi_1(x,y) \Pi_1(x+1,y) + H.c. \\
&= -i\epsilon \sum_{\boldsymbol{x}} (-1)^{s(\boldsymbol{x})} U_r(x,y) \xi_h(\boldsymbol{x}) (Z_r(x,y))^2 \Pi_1(x,y) \Pi_1(x+1,y) \\
&+ H.c. \\
&= -i\epsilon \sum_{\boldsymbol{x}} (-1)^{s(\boldsymbol{x})} U_r(x,y) G(\boldsymbol{x}) Z_d(x+1,y) Z_r(x,y) \\
&\times \Pi_1(x,y) \Pi_1(x+1,y) + H.c. \\
&= -\epsilon \sum_{\boldsymbol{x}} (-1)^{s(\boldsymbol{x})} Y_r(x,y) Z_d(x+1,y) \Pi_1(x,y) \Pi_1(x+1,y) + H.c. \\
&= -\epsilon \sum_{\boldsymbol{x}} (-1)^{s(\boldsymbol{x})} Y_r(x,y) Z_d(x+1,y) \Pi_1(x,y) \Pi_1(x+1,y) \\
&- \epsilon \sum_{\boldsymbol{x}} (-1)^{s(\boldsymbol{x})} Y_r(x,y) Z_d(x+1,y) \Pi_0(x,y) \Pi_0(x+1,y) \\
&= -\epsilon \sum_{\boldsymbol{x}} (-1)^{s(\boldsymbol{x})} Y_r(x,y) Z_d(x+1,y) \\
&\times \frac{1}{2}(1 + Z_u Z_l Z_d(x,y) \times Z_d Z_r Z_u(x+1,y))
\end{aligned}$$

In the step 1, the projection operators are collected, followed by insertion of $(Z_r(x,y))^2$ and simplification from the Gauss law constraint. In the last 3 steps, both terms are collected and Π_ρ values are inserted to give the final result.

Similarly the vertical interaction terms can be simplified as

$$\begin{aligned}
H_V &= -i\epsilon \sum_{\boldsymbol{x}} (-1)^{s(\boldsymbol{x})} \xi_v(\boldsymbol{x}) \Pi_{-1}(x,y) U_u(x,y) \Pi_1(x,y+1) + H.c. \\
&= -\epsilon \sum_{\boldsymbol{x}} (-1)^{s(\boldsymbol{x})} Y_u(x,y) Z_r(x,y) \\
&\times \frac{1}{2}(1 + Z_r Z_l Z_d(x,y) \times Z_l Z_r Z_u(x,y+1))
\end{aligned}$$

The interpretation of these terms is that, we will have an interaction term of form $Y \otimes Z$ acting when both

sites at the end of the links are empty or occupied. This corresponds to either particle-antiparticle pair creation or annihilation.

The pure gauge part of the Hamiltonian gets slightly altered, with the plaquette term becoming 6-local:

$$H_{KS} = H_E + H_B \tag{32}$$

$$= -2\lambda_E \sum_l Z_l - 2\lambda_B \sum_p Y_{p_1} Y_{p_2} X_{p_3} X_{p_4} Z_{p_5} Z_{p_6} \tag{33}$$

In this matter-eliminated formalism, the most complicated terms to implement are the interaction ones. They feature a controlled operation that is non-trivial only when both sites are empty or occupied. In the further sections we will show how these terms can be implemented with a better than expected circuit depth with re-using some of the occupation calculations. Despite the complications introduced by the projectors, the final gate complexity to perform time evolution is similar to using a fermion encoding method like Verstraete-Cirac encoding.

The same model was also considered in [11] where the authors arrived at the same result. In this work more emphasis is put towards optimization for circuit depth and comparison with other methods

E. Fermion encoding via VC transformation

Many other methods exist to deal with the fermion statistics in simulations. The simplest strategy that works well when working with 1D (or small 2D) systems is to encode the fermions via Jordan-Wigner transformation [22]. In this transformation, a particular ordering of fermions is assumed that allows to keep track of their CAR. However, in 2D there is no way to order the fermions in a way that would keep the interaction terms between neighbouring fermions of constant Pauli weight and in general the interaction terms will scale as $\mathcal{O}(L)$ where L is the linear size of the 2D system.

Alternatively, one of the fermion encoding methods that map a local fermion Hamiltonian to a local spin system [12, 23, 24] can be used. However, in all of these methods extra spins (qubits) are introduced to enforce the fermion CARs, thus making them unfavourable in terms of the spacial quantum computation requirements when compared to the fermion elimination method. The Verstraete-Cirac (VC) transformation [12] is a way how to encode fermions as spins by introducing ancillary qubits and encoding the fermionic statistics into this multi qubit increased Hilbert space via the mechanism of stabiliser codes. Despite the fact that this method has been around for nearly 2 decades it is still one of the lowest-weight encodings, and a gold standard for benchmarking [24].

In the VC approach, the pure gauge part of the Hamiltonian remains unchanged, with the matter part of Hamiltonian increasing in weight. To accommodate for fermion statistics, an extra qubit is introduced per each fermion site and they will be denoted by $\tilde{A}$. Under this mapping, the matter Hamiltonian becomes:

$$\begin{aligned}
H_f &= H_M + H_{int} \\
&= \sum_x \frac{(-1)^{s(\boldsymbol{x})} M}{2} Z(\boldsymbol{x}) + \\
&\sum_{\boldsymbol{x}} \epsilon_h(\boldsymbol{x}) X_r(\boldsymbol{x}) (X(x,y)X(x+1,y) \\
&+ Y(x,y)Y(x+1,y)) \tilde{Z}(\boldsymbol{x}) \\
&+ \sum_{\boldsymbol{x}} \epsilon_v(\boldsymbol{x}) X_u(\boldsymbol{x}) (X\tilde{Y}(x,y) Y\tilde{X}(x,y+1) \\
&- Y\tilde{Y}(x,y) X\tilde{X}(x,y+1))
\end{aligned}$$

Each of the horizontal terms have 2 components, each of weight 4 while the vertical components have weight 5.

III. QUANTUM CIRCUIT METHODS

A. Simulating time dynamics via Trotterization

Suzuki-Trotter method is a common way of simulating time dynamics. In this method the entire time evolution gets divided into $n = t/\delta$ steps of fixed size δ, as

$$U(t) = \exp(-iHt) = (\exp(-iH\delta))^{t/\delta}. \tag{34}$$

In general the Hamiltonian H contains multiple terms that do not commute. Such Hamiltonian can be written as $H = \sum_{i=1}^{\mathcal{M}} H_i$ where each H_i does not commute with the others, but all terms within each of them do. This allows one to approximate each step $U(\delta)$ as $\mathcal{V}(\delta)$:

$$U(\delta) \simeq \mathcal{V}(\delta) = \prod_{i=1}^{\mathcal{M}} \exp(-i\delta H_i) \tag{35}$$

In general a single Trotter step can be expressed as:

$$\mathcal{V}(\delta) = \prod_{i=M}^{1} (V_i R_i(\delta)) V_0 \tag{36}$$

where V_i is a general unitary operator and $R_i(\delta)$ is a Pauli operator rotation (in this case it can be controlled) that depends on the time step size δ. In further sections the exact form of each of the terms R_i, V_i will be given.

The entire error for the time evolution with Trotterization can be bound by [25]

$$\|U(t) - \mathcal{V}(t)\| \leq \frac{t^2}{2n} \sum_{i=1}^{\mathcal{M}} \left\| \sum_{j=i+1}^{\mathcal{M}} [H_i, H_j] \right\|$$

and the accuracy depends on the number of steps n. Furthermore, it has been observed that in practice these

bounds are loose and the Trotter error tends to be much smaller [25].

Recent studies [26, 27] that explored the chaos-regular transition in Trotterized quantum dynamics showed that even for large values of δ the systems still obey controlled behavior. Furthermore, the threshold for this transition is largely independent of the system size considered. This is an important result as it illustrates that one can faithfully probe time dynamics with large δ values, thus minimizing the number of steps and the circuit depth needed to perform a simulation of a given time. This strategy was already used to probe the fermionic $\mathbb{Z}_2$ theory in 1+1D in [19]. Here even values of $\delta \times \epsilon = 0.3$ were considered (where ϵ is the gauge-matter interaction strength).

B. Quantum Circuit for pure gauge $\mathbb{Z}_2$

In the pure $\mathbb{Z}_2$ case there are 2 non-commuting parts H_E and H_B. To perform time evolution we want to implement both $\exp(-i\delta H_E)$ and $\exp(-i\delta H_B)$. Implementing the $\exp(-i\theta H_E)$ is trivial in the chosen basis as it is just a Z rotation of the qubit $\exp(-i\theta Z)$:

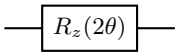

Implementing the terms in H_B is more difficult. Note that a weight K Pauli term can be implemented with $(2K-2)$ CX gates. For the terms appearing in H_B of form $\exp\left(i\theta X^{\otimes 4}\right)$, the identity $X_a X_b = CX_{ab} X_a CX_{ab}$ can be used to yield:

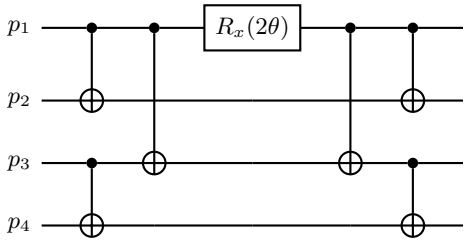

Thus, a single Trotter step of the pure theory can be implemented with $6 \times 1/2 \times L = (3 \times L)$ 2-qubit CX gates for a system with L links. A further simplification can be done if the middle 2 CX gates and the RX gate is combined into a CRX gate ($CRX_a(\theta) = CX_{ab} RX_a(\theta) CX_{ab}$).

C. Quantum Circuit for fermionic $\mathbb{Z}_2$

In the fermionic $\mathbb{Z}_2$ theory, we need to implement all 5 terms - H_E, H_B, H_M, H_H, H_V.

1. The implementation of the $\exp(-i\delta H_E)$ is the same as in the pure case, it consists of $\exp(-i\theta Z)$ rotations that can be done in parallel:

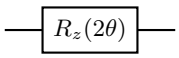

2. The implementation of $\exp(-i\delta H_B)$ is slightly more complicated than in the pure case as it is 6-local. Each term is of the form $\exp(-i\theta X_a X_b Y_c Y_d Z_e Z_f)$ and can be implemented as $V_2^\dagger RX_c(2\theta) V_2$ where the circuit V_2 is given by:

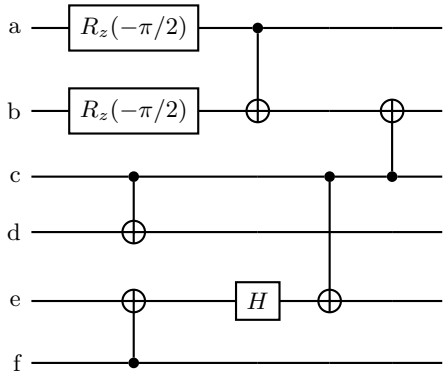

3. The evolution of the mass term $\exp(-i\delta H_M)$ is simply $\exp\left(-i\theta Z^{\otimes 4}\right)$ and can be implemented as $\exp\left(-i\theta Z^{\otimes 4}\right) = V_3^\dagger RZ_u(2\theta) V_3$ where V_3 is given by:

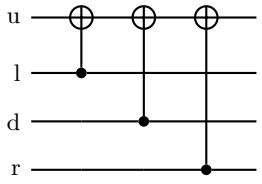

FIG. 2: The V_3 circuit can be interpreted as calculating the parity of the give vertex on link u

4. The horizontal interaction term evolution $\exp(-i\delta H_H)$, contains difficulties due to parity calculation and the fact the rotation that will be implemented is controlled. $\exp(-i\delta H_H) = V_4^\dagger CRZ_{(c,L)}(2\theta) V_4$ with V_4 given as:

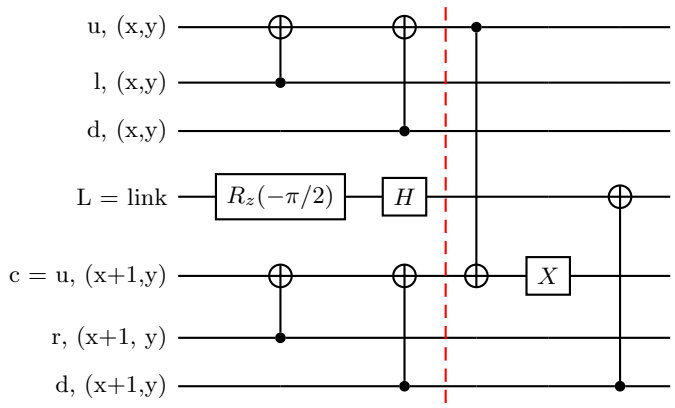

FIG. 3: Before the red line circuit calculates the relevant parity of each site and rotates the qubit L into Z basis, after the line we calculate the parity of both sites and perform the controlled rotation on L by c

5. The vertical interaction term is similar to the horizontal, making the structure of the circuit similar. Once again, $\exp(-i\delta H_V) = V_5^\dagger CRZ_{(c,L)}(2\theta)V_5$ with V_5 given as:

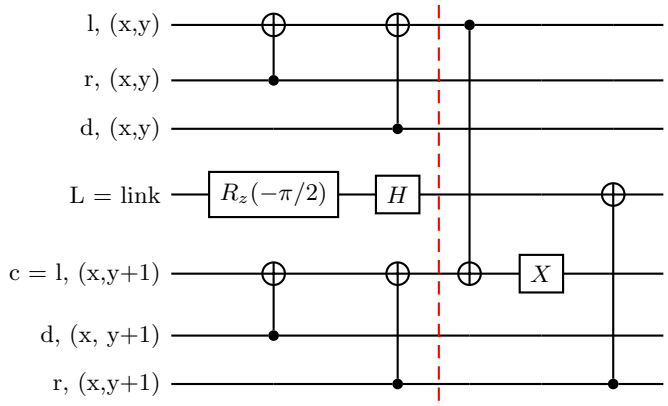

FIG. 4: Before the red line circuit calculates the relevant parity of each site and rotates the qubit L into Z basis, after the line we calculate the parity of both sites and perform the controlled rotation on L by c

Note that in all of the circuits the control gates act only between qubits that are nearest or next to nearest neighbours on the lattice.

If the ordering of the terms is chosen in an optimal way, it is possible to simplify the unitaries by contracting some of the CX gates into identities. Trivially, to apply all these terms one would need $10 \times 1/2L + 6 \times 1/2L + 12 \times L = 20L$ of CX gates and $1L$ of CR gate (Table I). By choosing this order optimally it can be brought down to $15L$ of CX and $1.5L$ of CR gates for L links.

This decomposition and simplification of the Hamiltonian is one of the main result in this work. A more detailed description of the optimal ordering to obtain this simplified result is given in the Appendix B.

The H term	Number of terms	Single cost	Total cost
H_E	L	0	0
H_B	L/2	10	5L
H_M	L/2	6	3L
H_H	L/2	12+1CRZ	6L + 0.5L CRZ
H_V	L/2	12+1CRZ	6L + 0.5L CRZ
Total			20 + 1CRZ

TABLE I: Table shows the cost of implementing each term of the Hamiltonian in terms of 2-qubit gates

Even though this fermion eliminated Hamiltonian has a complicated structure, the necessary number of 2 qubit gates is quite modest. In comparison, the Verstraete-Cirac method needs $10L$ CX and $2L$ CR gates. While the V-C method provides slightly lower circuit depth than the fermion elimination method, it require 2 times as many qubits to be implemented.

D. Approaches for circuit depth minimization

One possible way to decrease the circuit depth of a particular time dynamics simulation is to use variational methods, such as parametrized variational quantum dynamics (pVQD) [6]. The variational approaches allow one to decrease the circuit depth at the expense of executing the quantum circuit multiple times in the optimization subroutine.

In the pure $\mathbb{Z}_2$ theory, a Trotter step is given by

$$U(\delta) = \exp(-iH_B\delta)\exp(-iH_E\delta). \tag{37}$$

The full time evolution for time t can either be implemented by applying n Trotter steps such that $n\delta = t$, or approximated by a variational circuit. A good candidate for the variational circuit is to simply take k Trotter steps and variationally optimize the evolution parameters θ_i:

$$U_{var}(\vec{\theta}) = \prod_{j=1}^{k}(\exp(-iH_B\theta_{2j})\exp(-iH_E\theta_{2j+1})). \tag{38}$$

The optimization proceeds as follows:

1. Start with an easily preperable state $|\Psi\rangle$ to be evolved
2. For the first step maximize the overlap
$$\langle\Psi| U^\dagger(\vec{\theta^1})U(\delta)|\Psi\rangle \tag{39}$$
3. Denote the optimization parameters at step i as $\vec{\theta^{(i)}}$. Proceed to variationally maximize the overlap:
$$C(\vec{\theta}) = \langle\Psi| U^\dagger(\vec{\theta^{(i-1)}})U(\delta)U(\vec{\theta^{(i)}})|\Psi\rangle \tag{40}$$

by changing the parameters $\vec{\theta}^i$ and using the already optimized parameters from the previous timestep.

By saving the variational parameters $\vec{\theta}^{(i)}$ it is possible to implement the entire time evolution with the constant circuit depth of $2k+1$ (Trotter timesteps).

For the full fermionic theory, the ansatz can be constructed in a similar way:

$$U_{var}(\vec{\theta}) = \prod_{j=1}^{k} (\exp(-i\theta_{0+5j} H_B) \exp(-i\theta_{1+5j} H_E)) \exp\big(-i(-1)^{x+y}\theta_{2+5j} H_V\big) \exp(-i\theta_{3+5j} H_M) \exp\big(-i(-1)^{x+y}\theta_{4+5j} H_H\big)). \tag{41}$$

Even though here we only explore the application of the ansatz for simulating the time dynamics, it can also be used in variational algorithms like QAOA and VQE to probe the ground state properties of the system.

IV. NUMERICAL RESULTS

In this section we present the numerical results obtained using the methods introduced previously. Probing the time dynamics via Trotterization requires to repeat the single Trotter step circuit many times, which results in a large circuit depth and thus makes it hard to execute such simulations on NISQ. But the depth can be kept small and constant with the use of variational methods as pVQD, introduced in section III D. Here we explore this method when applied to both the pure gauge and the fermionic $\mathbb{Z}_2$ theories, focusing on a 2×2 lattice. We will explore how the accuracy depends on the number of Trotter layers used in ansatz (41). In all simulations we ignore the quantum noise that arises from measurements. We consider the evolution from the initial state

$$|\Psi_0\rangle = \prod_{1}^{L} |0\rangle \tag{42}$$

and measure the accuracy of the evolution by the fidelity of the pVQD approximation $\mathcal{F}$,

$$\mathcal{F}(t) = \left|\langle\Psi_0| \mathcal{V}^\dagger(t) U_{var}(\theta) |\Psi_0\rangle\right|^2. \tag{43}$$

The error of the approximation is $1 - \mathcal{F}(t)$.

A. Pure Gauge results

For the pure gauge theory with $g = 1$, figure 5 shows that the Trotterized evolution can be already very well approximated with an ansatz of depth $k = 2$, and this throughout the whole evolution considered. By using this method, it is possible to reduce circuit depth required from 20 to 5 Trotter steps. Furthermore, we find that the same value $k = 2$ can be used to probe the theory for other values of coupling constant g with similar success (Fig. 6). The agreement of the Trotterized and the exact results can be improved by decreasing the Trotter step size δ.

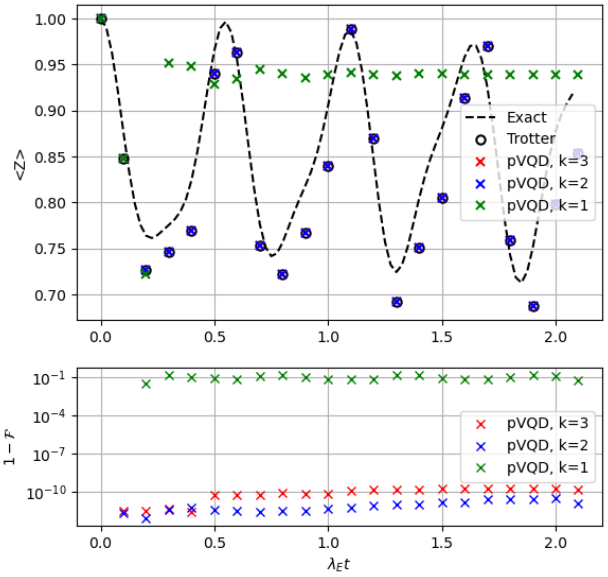

FIG. 5: The upper figure shows the time evolution of $\langle Z \rangle$ on a site, approximated with pVQD of depth $k = 1, 2, 3$ (crosses). For reference we show the results from the exact dynamics (dashed line) as well as the Trotterized one (circles). The bottom figure shows the errors associated with the evolution for each depth.

B. Full Fermionic results

The variational ansatz for the full fermionic theory consists of 5 terms compared to the 2 for the pure gauge case. This leads to the optimization process being slower and makes it more difficult to reach the global minimum. In this case we compare the results for depth values of $k = 1, 2$ along with their associated errors for the Hamiltonian with $(g, \epsilon, M) = (1, 0.2, 1)$ (Fig 7). In this case, the variational ansatz of depth $k = 2$ does not perform as well as in the pure gauge case, but still shows an improvement in the accuracy with respect to $k = 1$ for short times. The ansatz is able to perform the approximation just as well also in the stronger interaction case with $(g, \epsilon, M) = (1, 0.4, 1)$ (Fig. 8). Further increases in the ansatz depth should give more accurate results for longer time simulations.

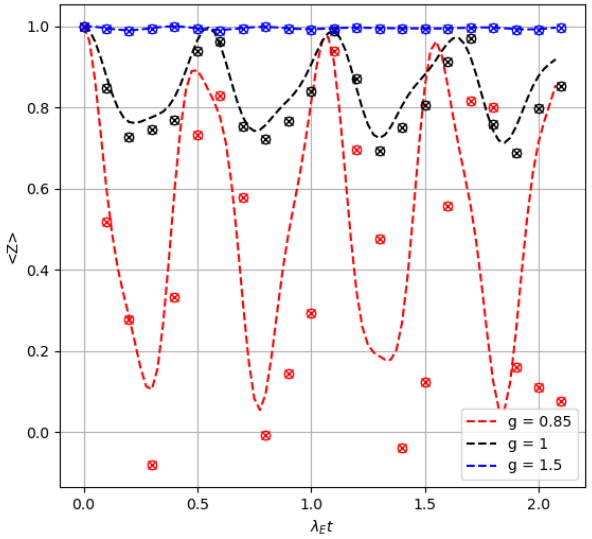

FIG. 6: The figure shows the pVQD results for $g = 0.85$, 1, 1.5. In this case the depth of $k = 2$ was used, leading to a 5-fold improvement in circuit depth when compared with the Trotterized evolution. As in figure 5, dashed lines and circles show, respectively, the results from the exact and Trotterized dynamics.

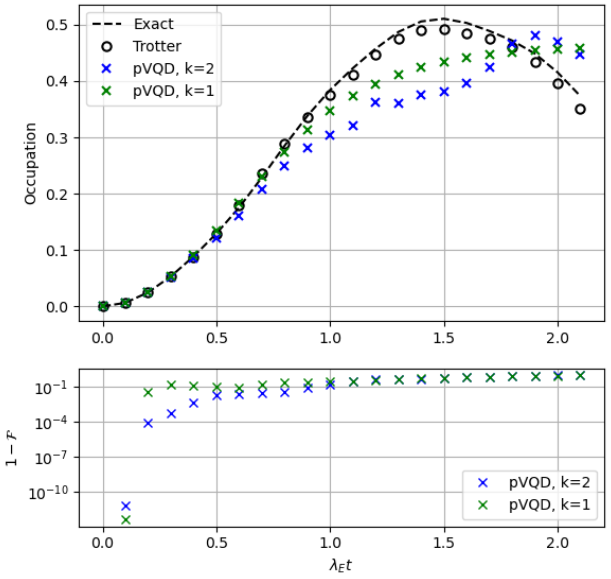

FIG. 7: The upper figure shows the results for the full fermionic theory for depth of $k = 1, 2$. The observable measured is the occupation of a site $n(0, 0)$. The lower plot shows the error values $1 - \mathcal{F}(t)$ associated with the evolutions for both depths.

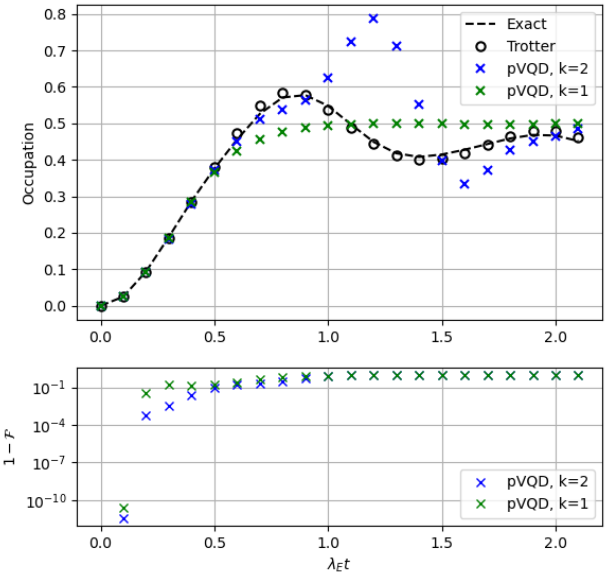

FIG. 8: The upper figure shows the results for the full fermionic theory for depth of $k = 1, 2$. The observable measured is the occupation of a site $n(0, 0)$. The lower plot shows the error values $1 - \mathcal{F}(t)$ associated with the evolutions for both depths. The agreement of the parametrized evolution is slightly worse than in the weaker interacting case (Fig 7)

V. CONCLUSION

Here we have presented a new method to simulate the full fermionic $\mathbb{Z}_2$ theory in (2+1) D with minimal resources, in particular, with minimal number of qubits. This was achieved by eliminating the fermionic degrees of freedom and absorbing them into the gauge field. For a lattice of size $M \times N$ one needs $L = 2 \times M \times N$ qubits (i.e. one per link) to simulate the model. In methods that involve encoding the fermions with the help of ancillary qubits, like the Verstraete-Cirac encoding [12], one needs twice as many qubits. Furthermore, the circuit depth was shown to be only slightly larger than for the alternative method (18 to 14 CX gates per link) and a variational Trotterization strategy (pVQD) was presented to further minimize it. Numerical results of the 2×2 lattice simulation suggest that the time dynamics of both the pure gauge and fermionic $\mathbb{Z}_2$ theory can be reasonably well approximated with Trotterized time dynamics. For the pure gauge theory, the pVQD performed exceptionally, by allowing to approximate $n = 20$ Trotter steps with only $k = 2$ steps in the variational ansatz. For the full fermionic case, the evolution can still be approximated by the variational ansatz, but the depth should be increased beyond $k = 2$ to obtain reliable re-

sults for longer times. This work shows that the fermion elimination method is an optimal approach for simulating the $\mathbb{Z}_2$ theory on a quantum computer, due to the minimal qubit requirements, and further improvements in the circuit depth that can be achieved by exploring the variational Trotterization methods. Further work involves developing similar methods for higher $\mathbb{Z}_N$ theories and extending them to (3+1) D.

While completing this manuscript, an independent proposal appeared that also explored the use of fermion elimination method for simulating the lattice gauge theories, including for the simulation of the fermionic $\mathbb{Z}_2$ in (2+1) D [11].

ACKNOWLEDGMENTS

This work was partially funded by the Deutsche Forschungsgemeinschaft (DFG, German Research Foundation) under Germany's Excellence Strategy – EXC-2111 – 390814868 and by the European Union through the ERC grant QUENOCOBA, ERC-2016-ADG (Grant no. 742102), and by the German Federal Ministry of Education and Research (BMBF) through EQUAHUMO (Grant No. 13N16066) within the funding program quantum technologies - from basic research to market and by the Munich Quantum Valley (MQV), which is supported by the Bavarian state government with funds from the Hightech Agenda Bayern Plus.

Appendix A: Quantum Circuit using the Verstraete Cirac encoding

The VC encoded Hamiltonian has $2L$ qubits as there are L qubits for the gauge field, $L/2$ fermions and $L/2$ extra ancillas.The Hamiltonian to simulate is $H = H_{KS} + H_f$ where we know that the terms in the pure gauge Hamiltonian H_{KS} can be simulated with $3L$ of CX gates per link. The H_f term is given as:

$$H_f = H_M + H_{int} \tag{A1}$$

$$= \sum_x \frac{(-1)^{s(\boldsymbol{x})} M}{2} Z(\boldsymbol{x}) + \tag{A2}$$

$$\sum_{\boldsymbol{x}} \epsilon_h(\boldsymbol{x}) X_r(\boldsymbol{x}) (X(x,y)X(x+1,y) \tag{A3}$$

$$+ Y(x,y)Y(x+1,y))\tilde{Z}(\boldsymbol{x}) \tag{A4}$$

$$+ \sum_{\boldsymbol{x}} \epsilon_v(\boldsymbol{x}) X_u(\boldsymbol{x}) (X\tilde{Y}(x,y)Y\tilde{X}(x,y+1) \tag{A5}$$

$$- Y\tilde{Y}(x,y)X\tilde{X}(x,y+1)) \tag{A6}$$

The mass term H_M can be implemented trivially since it is only an RZ gate.

The horizontal interaction term for each link has 2 weight-4 terms. For each of the terms we want to implement a rotation of type:

$$\exp(i\theta X_1 X_2 X_3 Z_4) \exp(i\theta X_1 Y_2 Y_3 Z_4)$$

Again, by using similar methods as before, this can be decomposed as:

$$\begin{aligned} &\exp(i\theta X_1 X_2 X_3 Z_4) \exp(i\theta X_1 Y_2 Y_3 Z_4) \\ &= H_4 \exp(i\theta X_1 X_2 X_3 X_4) RZ_2(-\pi/2) RZ_3(-\pi/2) \\ &\times \exp(i\theta X_1 X_2 X_3 X_4) RZ_2(\pi/2) RZ_3(\pi/2) H_4 \end{aligned}$$

which can be implemented with 6 CX gates and 2 CR gates. Similarly, the vertical interaction terms can be implemented with 8 CX and 2 CR gates.

Thus, the total cost for implementing a single step of Trotterized time evolution is $(3L + (6+8) \times L/2 = 10L)$ CX gates and $2L$ CR gates or $14L$ CX gates.

Appendix B: Ordering of the terms

The optimal way of ordering the terms, to reduce the 2 qubit gate count is given here.

1. Perform the evolution of H_E on all links
2. Perform the evolution of H_B first on (x,y) = (even,even), followed by (odd,even). The plaquettes location is described by the vertex where all 4 surrounding links are involved
3. Perform the H_H on (x,y) = (even,even)
4. Perform H_M on (x,y) = (all,even)
5. Perform H_H on (x,y) = (odd,even)
6. Perform H_V on (x,y) = (even,even) followed by (even,odd)
7. Perform H_V on (x,y) = (odd,odd) followed by (odd,even)
8. Perform H_H on (x,y) = (even,odd)
9. Perform H_M on (x,y) = (all,odd)
10. Perform H_H on (x,y) = (odd,odd)
11. Perform H_B on (x,y) = (even,odd) followed by (odd,odd)

The possible simplification that can be done here are not fully uncomputing/computing the parity of the vertex between different interaction/mass terms and altering the unitary V_2 to allow calculating the parity of the vertex as the H_B term is being uncomputed/computed.

[1] Andrew M. Childs, Dmitri Maslov, Yunseong Nam, Neil J. Ross, and Yuan Su. Toward the first quantum simulation with quantum speedup. *Proceedings of the National Academy of Sciences of the United States of America*, 115(38):9456–9461, 2018.

[2] Bela Bauer, Sergey Bravyi, Mario Motta, and Garnet Kin-Lic Chan. Quantum Algorithms for Quantum Chemistry and Quantum Materials Science. *Chemical Reviews*, 120(22):12685–12717, 2020.

[3] Laura Clinton, Toby Cubitt, Brian Flynn, Filippo Maria Gambetta, Joel Klassen, Ashley Montanaro, Stephen Piddock, Raul A. Santos, and Evan Sheridan. Towards near-term quantum simulation of materials. 2022.

[4] M. C. Banuls, R. Blatt, J. Catani, A. Celi, and J. I. Cirac. Simulating Lattice Gauge theories. *The European Physics Journal D*, 2020.

[5] Frank Arute, Kunal Arya, Ryan Babbush, Dave Bacon, Joseph C. Bardin, Rami Barends, Rupak Biswas, Sergio Boixo, Fernando G.S.L. Brandao, David A. Buell, Brian Burkett, Yu Chen, Zijun Chen, Ben Chiaro, Roberto Collins, William Courtney, Andrew Dunsworth, Edward Farhi, Brooks Foxen, Austin Fowler, Craig Gidney, Marissa Giustina, Rob Graff, Keith Guerin, Steve Habegger, Matthew P. Harrigan, Michael J. Hartmann, Alan Ho, Markus Hoffmann, Trent Huang, Travis S. Humble, Sergei V. Isakov, Evan Jeffrey, Zhang Jiang, Dvir Kafri, Kostyantyn Kechedzhi, Julian Kelly, Paul V. Klimov, Sergey Knysh, Alexander Korotkov, Fedor Kostritsa, David Landhuis, Mike Lindmark, Erik Lucero, Dmitry Lyakh, Salvatore Mandrà, Jarrod R. McClean, Matthew McEwen, Anthony Megrant, Xiao Mi, Kristel Michielsen, Masoud Mohseni, Josh Mutus, Ofer Naaman, Matthew Neeley, Charles Neill, Murphy Yuezhen Niu, Eric Ostby, Andre Petukhov, John C. Platt, Chris Quintana, Eleanor G. Rieffel, Pedram Roushan, Nicholas C. Rubin, Daniel Sank, Kevin J. Satzinger, Vadim Smelyanskiy, Kevin J. Sung, Matthew D. Trevithick, Amit Vainsencher, Benjamin Villalonga, Theodore White, Z. Jamie Yao, Ping Yeh, Adam Zalcman, Hartmut Neven, and John M. Martinis. Quantum supremacy using a programmable superconducting processor. *Nature*, 574(7779):505–510, oct 2019.

[6] Stefano Barison, Filippo Vicentini, and Giuseppe Carleo. An efficient quantum algorithm for the time evolution of parameterized circuits. *Quantum*, 5, jan 2021.

[7] Refik Mansuroglu, Samuel Wilkinson, Ludwig Nützel, and Michael J. Hartmann. Classical Variational Optimization of Gate Sequences for Time Evolution of Large Quantum Systems. jun 2021.

[8] Cristina Cîrstoiu, Zoë Holmes, Joseph Iosue, Lukasz Cincio, Patrick J. Coles, and Andrew Sornborger. Variational fast forwarding for quantum simulation beyond the coherence time. *npj Quantum Information*, 6(1), 2020.

[9] Erez Zohar and J. Ignacio Cirac. Eliminating fermionic matter fields in lattice gauge theories. *Physical Review B*, 98(7), aug 2018.

[10] Erez Zohar and J. Ignacio Cirac. Removing staggered fermionic matter in U (N) and SU (N) lattice gauge theories. *Physical Review D*, 99(11), jun 2019.

[11] Tomer Greenberg, Guy Pardo, Aryeh Fortinsky, and Erez Zohar. Resource-Efficient Quantum Simulation of Lattice Gauge Theories in Arbitrary Dimensions: Solving for Gauss' Law and Fermion Elimination. 2022.

[12] F. Verstraete and J. I. Cirac. Mapping local Hamiltonians of fermions to local Hamiltonians of spins. *Journal of Statistical Mechanics: Theory and Experiment*, (9):305–314, sep 2005.

[13] S. Dürr, Z. Fodor, J. Frison, C. Hoelbling, R. Hoffmann, S. D. Katz, S. Krieg, T. Kurth, L. Lellouch, T. Lippert, K. K. Szabo, and G. Vulvert. Ab initio determination of light hadron masses. *Science*, 322(5905):1224–1227, nov 2008.

[14] Claudia Ratti. Lattice QCD and heavy ion collisions: A review of recent progress. *Reports on Progress in Physics*, 81(8), 2018.

[15] Ryu Ikeda and Kei Ichi Kondo. Center group dominance in quark confinement. *Progress of Theoretical and Experimental Physics*, 2021(10):0, jun 2021.

[16] Lukas Homeier, Christian Schweizer, Monika Aidelsburger, Arkady Fedorov, and Fabian Grusdt. Z2 lattice gauge theories and Kitaev's toric code: A scheme for analog quantum simulation. *Physical Review B*, 104(8), dec 2021.

[17] Luca Lumia, Pietro Torta, Glen B. Mbeng, Giuseppe E. Santoro, Elisa Ercolessi, Michele Burrello, and Matteo M. Wauters. Two-Dimensional Z 2 Lattice Gauge Theory on a Near-Term Quantum Simulator: Variational Quantum Optimization, Confinement, and Topological Order . *PRX Quantum*, 3(2), 2022.

[18] Erik J. Gustafson and Henry Lamm. Toward quantum simulations of Z2 gauge theory without state preparation. *Physical Review D*, 103(5):054507, mar 2021.

[19] Julius Mildenberger, Wojciech Mruczkiewicz, Jad C. Halimeh, Zhang Jiang, and Philipp Hauke. Probing confinement in a Z2 lattice gauge theory on a quantum computer. 2022.

[20] John Kogut and Leonard Susskind. Hamiltonian formulation of Wilson's lattice gauge theories. *Physical Review D*, 11(2):395–408, 1975.

[21] Gyan Bhanot and Michael Creutz. Phase diagram of Z(N) and U(1) gauge theories in three dimensions. Technical Report 10, 1980.

[22] P. Jordan and E. Wigner. Über das Paulische Äquivalenzverbot. *Zeitschrift für Physik*, 47(9-10):631–651, 1928.

[23] Mark Steudtner and Stephanie Wehner. Quantum codes for quantum simulation of fermions on a square lattice of qubits. *Physical Review A*, 99(2), feb 2019.

[24] Charles Derby, Joel Klassen, Johannes Bausch, and Toby Cubitt. Compact fermion to qubit mappings. *Physical Review B*, 104(3), 2021.

[25] Andrew M. Childs, Yuan Su, Minh C. Tran, Nathan Wiebe, and Shuchen Zhu. Theory of Trotter Error with Commutator Scaling. *Physical Review X*, 11(1), 2021.

[26] Markus Heyl, Philipp Hauke, and Peter Zoller. Quantum localization bounds Trotter errors in digital quantum simulation. *Science Advances*, 5(4), 2019.

[27] Karthik Chinni, Manuel H. Muñoz-Arias, Ivan H. Deutsch, and Pablo M. Poggi. Trotter Errors from Dynamical Structural Instabilities of Floquet Maps in Quantum Simulation. *PRX Quantum*, 3(1), oct 2022.